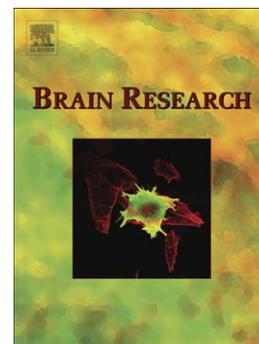# Accepted Manuscript

Modulation of blood-brain barrier permeability by neutrophils: in vitro and in vivo studies

Shannon L. Joice, Firdaus Mydeen, Pierre-Olivier Couraud, Babette B. Weksler, Ignacio A. Romero, Paul A. Fraser, Alexander S. Easton

Please cite this article as: Shannon L. Joice, Firdaus Mydeen, Pierre-Olivier Couraud, Babette B. Weksler, Ignacio A. Romero, Paul A. Fraser, Alexander S. Easton, Modulation of blood-brain barrier permeability by neutrophils: in vitro and in vivo studies, *Brain Research* (2009), doi:10.1016/j.brainres.2009.08.076

Modulation of blood-brain barrier permeability by neutrophils: in vitro and in vivo studies.

Shannon L Joice[1], Firdaus Mydeen[1], Pierre-Olivier Couraud[4,5,6,7], Babette B Weksler[5,8], Ignacio A Romero[9], Paul A Fraser[10] & Alexander S Easton[1,2,3].

1. Department of Pathology, Dalhousie University, Halifax, Nova Scotia, Canada.

2. Department of Microbiology and Immunology, Dalhousie University, Halifax, Nova Scotia, Canada.

3. Division of Neurosurgery, Department of Surgery, Dalhousie University, Halifax, Nova Scotia, Canada.

4. Department of Cell Biology, Institut Cochin, Paris, France.

5. Inserm, U567, Paris, France.

6. CNRS, UMR 8104, Paris, France.

7. Université Paris 5, Faculté de Médecine René Descartes, UM3, Paris, France.

8. Department of Medicine, Weill Medical College, New York, New York, USA.

9. Department of Biological Sciences, The Open University, Milton Keynes, UK.

10. Cardiovascular Division, King's College London, London, UK.

Pages: 33, Figures: 5

Corresponding author:

Dr Alexander S Easton

Department of Pathology, Dalhousie University

Sir Charles Tupper Medical Building, Room 11J

5850 College Street, Halifax, Nova Scotia, Canada B3H 1X5

Email Alexander.Easton@dal.ca

Tel 902 473 8255

Fax 902 473 7978

Abstract.

The blood-brain barrier (BBB) restricts solute permeability across healthy cerebral endothelial cells. However, during inflammation, permeability is increased and can lead to deleterious cerebral edema. Neutrophils are early cellular participants in acute inflammation, but their effect on BBB permeability is unclear. To study this, neutrophils were applied in a resting and activated state to in vitro and in vivo models of the BBB. In vitro, human neutrophils (5 X 10^6/ml) were activated with tumor necrosis factor (100U/ml) and leukotriene B_4 (10^{-7}mol/l). Untreated neutrophils reduced permeability across the human brain endothelial cell line hCMEC/ D3. Activated neutrophils returned permeability to baseline, an effect blocked by the reactive oxygen scavengers superoxide dismutase (10U/ml) and catalase (1000U/ml). In vivo, human neutrophils (2.5 X 10^5 in 4μl) were injected into the striatum of anesthetized juvenile Wistar rats, and BBB permeability measured 30 minutes later. This was compared to control injections (4μl) of vehicle (0.9% saline) and arachidonic acid (10^{-3}mol/l). The injection generated a small hematoma around the injection tract (<3μl). Untreated neutrophils induced significantly lower permeability in their vicinity than activated neutrophils, with a trend to lowered permeability compared to the vehicle control. Neither untreated nor activated neutrophils induced permeability increases, while arachidonic acid increased permeability as a positive control. This study further delineates the effect of neutrophils on the BBB, and demonstrates that resting neutrophils induce acute reductions in permeability while activated neutrophils have a neutral effect. The in vivo model reiterates some aspects of acute intracerebral hemorrhage.

Section: Cellular and molecular biology of nervous systems.

Keywords: blood-brain barrier, neutrophil, inflammation, hemorrhage.

1. Introduction.

The blood-brain barrier (BBB) is a term used to describe a low permeability to hydrophilic

solutes across the endothelial cells that line cerebral microvessels (Reese & Karnovsky, 1967).

In health, the BBB preserves the ionic composition of the brain interstitium, necessary for

normal neuronal function. However, during inflammation, BBB permeability is increased. One

consequence of this is the extravasation of plasma proteins into the brain, with net retention of

brain water (Simard et al, 2007). The subsequent tissue edema is clinically deleterious,

contributing to the morbidity and mortality in acute inflammatory diseases of the central nervous

system (CNS) such as hemorrhagic and ischemic stroke, meningitis and head injury. This

vasogenic form of cerebral edema is difficult to treat, and its pathogenesis is incompletely

understood.

Neutrophils are white blood cells that act as early cellular participants in acute cerebral

inflammation. The inflammatory state causes activation of cerebral endothelial cells, leading to

the adhesion and transmigration of neutrophils through the endothelial barrier into the tissues.

Neutrophils may also extravasate directly into the brain following an acute hemorrhage without

first undergoing transmigration. Neutrophils undergo a process of activation in response to

inflammatory factors, which includes activation of NADPH oxidase and generation of reactive

oxygen species (ROS) such as superoxide, which have been implicated as mediators of BBB

permeability increases. At any of these stages (neutrophil-endothelial interactions,

transmigration, direct tissue effects and activation) neutrophils may therefore impact on the BBB

and potentially contribute to vasogenic edema.

Where neutrophils have been studied in animal models of CNS disease, results have been conflicting. For instance, the time over which neutrophils infiltrate an ischemic stroke (beginning at 6h in experimental studies in the rat (Barone et al, 1995) and 15h in humans (Lindsberg et al, 1996) and persisting for days) mirrors edema development, suggesting that neutrophils could be causal factors (Lindsberg et al, 1996; Zhang et al, 1994, Del Zoppo et al, 2001). However studies in animal disease models have been contradictory, with some correlating neutrophils to indicators of brain edema (Del Maschio et al, 1999; Matsuo et al, 1994; Wispelwey et al, 1988; Yamasaki et al, 1995). Others show no relationship (Adelson et al, 1998; Hartl et al, 1997; Tauber et al, 1988; Whalen et al, 1999) while others suggest that neutrophils reduce BBB disruption (Ahmed et al, 2000; Lo et al, 1998; Schurer et al, 1990).

The contradictory findings of these studies may perhaps be explained by the numerous variables that operate between models. It is not clear whether neutrophils are activated, what mediators they secrete or at what anatomical level they operate, for instance by occluding microvessels with subsequent reperfusion injury or acting from within the tissues on a variety of cellular components (neurons, glia etc). Another approach is to apply neutrophils directly to models of the BBB. Previous work carried out by our group determined that untreated neutrophils (untreated in the sense that inflammatory factors were not applied to induce neutrophil activation) reduce permeability across an in vitro model of the BBB made up of cerebral endothelial cells. When neutrophils were induced to migrate through the endothelial barrier they tended to return the permeability to baseline without inducing net permeability increases (Inglis et al, 2004). This may function to preserve the integrity of the BBB during neutrophil diapedesis. In vivo studies have increased neutrophil infiltration through stereotactic injections

5

of cytokines (interleukin 1-β) or chemokines (cytokine induced neutrophil chemoattractant-1) into the previously normal brain. Particularly in juvenile rats, these agents induced a major neutrophil dependent increase in BBB permeability (Anthony et al, 1997; 1998). However it is not clear if these effects would differ in an inflammatory setting. Also, neutrophils are admixed with the other components of blood and so enter the brain directly in the early stages of acute intracerebral hemorrhage, where they may have different effects.

The approach we have adopted in this study is to apply neutrophils directly to a simplified model of cerebral endothelial cells in vitro, and to inject them directly into the CNS parenchyma in vivo, with determinations of BBB permeability. We principally wished to contrast the effects of untreated versus activated neutrophils on BBB permeability, measured 30min after application. It was not our intention to extensively model any particular CNS disease, however the in vivo model can be taken to mimic the early stages of neutrophil extravasation into an acute intracerebral hemorrhage (hemorrhagic stroke).

2. Results.

Permeability across the human brain endothelial cell line hCMEC/D3.

hCMEC/D3 are a cell line derived by immortalizing human primary brain endothelial cells with telomerase and SV40 large T antigen (Weksler et al, 2005). In order to compare their responses to other cell culture models of the BBB, hCMEC/D3 cells were treated with agents reported to reduce or increase permeability (Rubin et al, 1991; Easton & Fraser, 1998). Baseline permeability across untreated monolayers, calculated from the clearance of 4kd FITC dextran, was $7.99 \pm 0.73 \times 10^{-4}$ cm/min (mean ± standard error of the mean). In one set of experiments, cells were pre-treated for 24h with a combination of dibutyryl cyclic AMP (dbcAMP, 2.5×10^{-4} mol/l) and rolipram, a selective phosphodiesterase 4 antagonist that inhibits intracellular cAMP degradation (1.75×10^{-5} mol/l). This treatment significantly reduced permeability below baseline to $4.53 \pm 0.31 \times 10^{-4}$ cm/min. In other experiments, cells were treated acutely with arachidonic acid (0.5×10^{-3} mol/l) which significantly increased permeability to $18.99 \pm 3.81 \times 10^{-4}$ cm/min (fig 1).

Figure 1 near here

The effect of neutrophil activation on permeability across hCMEC/D3.

Neutrophil activation involves the production of reactive oxygen species (ROS) in response to external stimuli. Superoxide is generated by neutrophil NADPH oxidase, an enzyme that requires preassembly at the plasma membrane prior to full activation. To activate neutrophils, they were treated with tumor necrosis factor (TNF) and leukotriene B_4 (LtB$_4$). TNF has been shown to induce preassembly of NADPH oxidase, which enhances superoxide production by

neutrophils in response to LtB$_4$ (Palmblad et al, 1984; Berkow et al, 1987; Sheppard et al, 2005). To confirm activation, an in vitro assay was carried out. ROS production was measured by loading neutrophils with carboxy-2',7'-dichlorodihydrofluorescein diacetate (carboxy-H$_2$DCFDA). The change in carboxy-H$_2$DCFDA fluorescence over a 135 minute observation period is shown in fig 2A. The vehicle control (phosphate buffered saline, PBS) did not alter fluorescence. Untreated neutrophils generated an increase in fluorescence, significantly greater than vehicle alone (P<0.001). Compared to untreated neutrophils, fluorescence did not increase when neutrophils were pre-treated for 1h with TNF (100U/ml). However treatment with LtB$_4$ (1 X 10^{-7} mol/l) alone or following TNF pre-treatment significantly increased fluorescence, both to comparable levels. Treatment with phorbyl 12-myristate, 13-acetate (PMA, 4 X 10^{-8}mol/l) induced an increase in fluorescence that was significantly greater than LtB$_4$ (P<0.001), which was blocked in combination with the NADPH oxidase inhibitor diphenylene iodinium chloride (DPI, 8 X 10^{-6} mol/l).

Neutrophils were then applied to hCMEC/D3 to determine their effects on permeability (fig 2B). Permeability is expressed as a percentage of the mean permeability across untreated monolayers measured concurrently (% of baseline). Baseline permeability across the untreated inserts used in these experiments was 6.02 ± 0.44 X 10^{-4}cm/min (n=18). Untreated neutrophils were applied above the monolayers at a density of 5 X 10^6/ml, which reflects neutrophil counts in whole blood (4-11 X 10^6/ml). We previously observed that it took 30min to see maximum changes in permeability (Inglis et al, 2004) so neutrophils were left for 30min before permeability was measured. Untreated neutrophils reduced permeability to 47.67 ± 2.57 % of baseline (n=7), a significant reduction. However, when neutrophils were exposed to a gradient of LtB$_4$ (10^{-7}mol/l)

applied below the cells, permeability increased to 86.78 ± 10.60 % of baseline (n=9),

significantly greater than untreated neutrophils and not different from baseline. To activate

neutrophils, they were pre-treated with 100U/ml TNF for 1h. TNF was then removed by

washing, and neutrophils resuspended in fresh medium before application, to avoid additional

effects of TNF on permeability. LtB_4 (1×10^{-7}mol/l) was then applied first above and then

below the monolayers, to avoid a gradient. The resulting permeability was both significantly

greater than untreated neutrophils, and not significantly different from baseline (81.42 ± 3.03%

of baseline, n=12). However, this effect was blocked by the combined ROS scavengers

superoxide dismutase (10U/ml) and catalase (1000U/ml), in whose presence permeability was

significantly reduced below baseline, and not significantly different from untreated neutrophils

(56.97 ± 2.95 % of baseline, n=12). To determine if LtB_4 increases permeability independent of

neutrophils, permeability was measured following application of LtB_4 alone. This did not result

in significant differences compared to baseline (97.85 ± 10.56 % of baseline, n=15).

Figure 2 near here

In vivo changes in permeability around a striatal injections of neutrophils.

Permeability was measured around striatal injections in anesthetized juvenile Wistar rats. The

negative control contained vehicle alone (0.9% saline). The three other injectates contained

untreated neutrophils (2.5×10^5 per injection), activated neutrophils and arachidonic acid (1×10^{-3}mol/l). Activated neutrophils were pre-treated with Tumor necrosis factor (TNF) prior to

injection (100U/ml, 1h). TNF was removed by washing before neutrophils were injected.

Following injection, Leukotriene (Lt)B_4 was injected intravenously (variable doses in 200µl

9

saline) to give an estimated circulating concentration of 10^{-7}mol/l, based on dilution in a

circulating volume estimated at 7% rat body weight. This circulated for 15min prior to

intravascular infusion of HRP used as the in vivo permeability tracer. These factors were chosen

to mimic the activation conditions used in vitro. The injection procedure induced a small

hematoma in the injection tract, whose volume was measured by image analysis. In the saline

injected group the volume was $1.09 \pm 0.23\mu l$ (mean± sem, range: 0.25-2.67µl, n=10 rats). The

volume around untreated neutrophils was $0.67 \pm 0.09\mu l$ (0.32-1.48µl, n=15 rats) while that

around activated neutrophils was $0.89 \pm 0.12\mu l$ (0.45-1.48µl, n=9 rats). There were no

statistically significant differences in hematoma volume between the groups. Examples of the

appearance of the injection site and of how permeability maps were constructed around it are

shown in figure 3. Fig 3A shows activated neutrophils, while fig 3B shows an area adjacent to

the injection site for arachidonic acid. Upper and lower panels show the 30µm sections (H&E)

immediately anterior and posterior to the 120µm section that was processed to generate a

permeability map (middle panel), in which pixels have been pseudocolored to indicate regional

differences in permeability-surface area (PS) product. In fig 3A, the permeability map shows a

linear region of increased permeability in the vicinity of the hematoma. Fig 3B shows dilated

microvessels in the vicinity of arachidonic acid (H&E sections), while there are multiple regions

of increased permeability discernable in the permeability map.

Figure 3 near here

Average PS was calculated in contiguous regions of interest in the vicinity of the injection site.

For example, one region would be analyzed in fig 3A, with multiple regions analyzed in fig 3B.

10

PS values were then averaged for all the regions of interest in each rat, to obtain a single value of PS per rat. Multiple values, each one derived from a separate rat, were averaged to obtain PS values for each treatment group, shown in figure 4. PS increased around the saline vehicle to $112.37 \pm 39.06 \times 10^{-6}$ ml/s/g. In comparison, the PS reduced around untreated neutrophils (to $59.03 \pm 26.97 \times 10^{-6}$ ml/s/g) however the reduction was not statistically significant. The PS around activated neutrophils ($89.90 \pm 23.27 \times 10^{-6}$ ml/s/g) was also not significantly different from saline, and there was no significant difference between untreated and activated neutrophils. The PS around arachidonic acid increased to $499.28 \pm 94.79 \times 10^{-6}$ ml/s/g, which was significantly increased over all other groups ($P<0.05$ compared to activated neutrophils and saline, $P<0.001$ compared to untreated neutrophils).

Figure 4 near here

The data is also expressed as PS values from all regions of interest in the permeability maps, pooling the data from all of the rats. This is shown as histograms for each treatment group in figure 5. Values around untreated neutrophils were significantly reduced compared to activated neutrophils ($X^2=13.98$, $P<0.01$). Both activated and untreated neutrophils were not significantly different from the saline group. However, arachidonic acid was significantly greater than saline ($X^2=107.04$, $P<0.001$).

Figure 5 near here

11

3. Discussion.

Summary of findings.

BBB permeability was measured 30 minutes after application of neutrophils (untreated or activated) to in vitro and in vivo models. The in vitro model employed the human brain endothelial cell line hCMEC/D3. When human neutrophils (5×10^6/ml) were applied to the monolayers, untreated cells induced significant reductions in permeability. Subsequent activation with TNF (100U/ml) and LtB_4 (10^{-7}mol/l) increased permeability relative to the untreated neutrophils, but did not increase permeability over baseline. This increase was mediated by reactive oxygen species (ROS), as it could be blocked with the combined ROS scavengers superoxide dismutase (10U/ml) and catalase (1000U/ml). The in vivo model employed direct striatal injections of neutrophils (2.5×10^5 in 4μl) using a 26 gauge metal needle that also generated acute hemorrhage in the needle tract (final volume under 3μl). Neutrophils were either untreated or activated by TNF pretreatment and administration of intravenous LtB_4 at the doses used in vitro. Permeability was also assessed at 30min in the animal model. The injection procedure and associated hemorrhage generated an increase in BBB permeability around the vehicle control. The introduction of untreated neutrophils into the injection field reduced permeability compared to activated neutrophils (fig 5) with a trend to a reduction compared to vehicle (fig 4). However, permeability around activated neutrophils was not different from the vehicle control. The data show that untreated neutrophils reduce BBB permeability while activated neutrophils have neutral effects, whether they are applied in vitro or in vivo.

In vitro model of the BBB.

hCMEC/D3 cells are derived by immortalization of human brain primary endothelial cells using SV40 large T antigen and telomerase (Weksler et al, 2005). The advantage of using hCMEC/D3 cells is that they model the human BBB, express a number of properties of the in situ BBB, maintain those properties reliably over several passage numbers, and avoid the inherent variability as well as the difficulty of sourcing that apply to human primaries. The cells mimic the changes in permeability across the BBB that occur in situ in response to inflammatory mediators. We show that arachidonic acid applied at the same concentration used in vivo, induced a significant increase in permeability as a positive control, while treatment of hCMEC/D3 to enhance levels of intracellular cyclic AMP reduced permeability as a negative control (fig 1). This data provides further validation for using hCMEC/D3 to model changes in BBB permeability. Dextran clearance was chosen to measure permeability, based on the initial description of hCMEC/D3. This study (Weksler et al, 2005) showed that use of dextran generated permeability values that were comparable to primary bovine brain endothelial cultures. Like Weksler et al (2005), we found that transendothelial electrical resistance was too low in the monolayers (baseline under $30\Omega.cm^2$) to permit this to be used to measure the permeability. This appears to relate to the static conditions of the assay rather than a deficiency in the cell line as such, since TEER can be increased when cells are exposed to shear stress (Cucullo et al, 2008) or grown in serum free medium supplemented with hydrocortisone (Forster et al, 2008). While fluorescent dextrans are useful for the in vitro model, we used a different marker for the in vivo study. The use of HRP was partly dictated by the method described by Gauden et al (2007). We were also concerned that fluorescent dyes in brain slices can prove unreliable, since in tissue

stored for several days the fluorescent label could dissociate from the tracer molecule, and during processing its intensity could reduce through photobleaching.

There was similarity between the in vitro and in vivo findings. When untreated neutrophils were applied to the hCMEC/D3 monolayers, they induced a significant reduction in permeability 30min after application. We did not explore the mechanism, but our previous work (Inglis et al, 2004) showed that neutrophils reduce permeability through adenosine and ROS. Treatment with TNF and LtB_4 resulted in generation of ROS, assessed in an independent assay (fig 2A). The assay has limitations, because the dye used is intracellular and so may not detect most of the superoxide released extracellularly by the activated neutrophils. This may explain why TNF treatment appeared not to potentiate ROS production in response to LtB_4. However, these activation conditions negated the permeability reduction seen with the untreated neutrophils, but without raising permeability above baseline. This small increase in permeability back to baseline was blocked with the ROS scavengers catalase and superoxide dismutase. It is of interest that ROS reduce permeability when untreated neutrophils are applied to brain endothelial monolayers (Inglis et al, 2004), but mediate small increases in permeability when neutrophils are activated. Other in vitro studies have demonstrated that neutrophils increase permeability during migration across cultured primary brain endothelium, both bovine (Inglis et al., 2004) and human (Wong et al, 2007). However, our previous work (Inglis et al, 2004) suggests that neutrophils also reduce permeability in the period preceding migration, so that little net increase occurs. This was reproduced in this study when untreated neutrophils were applied to human hCMEC/D3 monolayers followed by a chemotactic gradient of LtB_4 that would be expected to induce transmigration (fig 2B).

14

In vivo model of the BBB.

The use of direct injections of leucocytes into the brain is not an entirely novel approach, as it has been employed in studies of acute intracerebral hemorrhage (Xue and Del Bigio, 2000). We chose to assess the impact of injected neutrophils after 30min to match our observations with those of the in vitro model (fig 2). Also, in order to optimize the effect of neutrophil activation, LtB$_4$ was injected intravenously after the neutrophils were injected. As LtB$_4$ is lipid soluble, we expected it to gain ready access to the brain. In previous work on single pial microvessels in the same age and species of rat, we had observed that 10^{-7}mol/l LtB$_4$ does not itself alter permeability (A Easton, unpublished observation). By injecting neutrophils directly into the brain we were mimicking the effect of extravasated neutrophils, admixed with the other blood components that enter the tissue in the earliest stages of acute intracerebral hemorrhage. This makes the method relevant to a pathophysiological situation in which inflammation plays a part, however it was not our intention to examine this exhaustively. In acute intracerebral hemorrhage, injury to the BBB develops over a period of several hours, peaking at 48h in the rat. Also, this is associated with endogenous neutrophils that take several hours to diapedese into the injured brain, and cerebral edema develops around larger hematomas than that generated in this study, of the order of 100μl in experimental models of acute intracerebral hemorrhage in the rat (Jenkins et al, 1989; Kitaoka et al, 2002). Therefore we have not modeled several aspects of acute intracerebral hemorrhage including the role of neutrophils at later times after injury, and their effect on larger hematomas which are more clinically relevant in terms of edema formation. However, this study does show that extravasated neutrophils can reduce early injury to the BBB around a small hematoma. A recent paper (Keep et al, 2005) discusses the role of neutrophils (as well as other factors) in the pathogenesis of acute intracerebral hemorrhage, and suggests that

they might have beneficial effects in small hematomas (under 50μl in the rat) but have detrimental effects in larger hematomas. This is a concept supported by our data. It is possible that neutrophils administered to a larger hematoma, or at later times in a model of acute intracerebral hemorrhage would not have reduced the permeability.

In the rat, significant injury is induced when 100μl of whole blood is injected into the striatum (Kitaoka et al, 2002). The true relative blood volume of leucocytes in this volume of blood is about 4μl. The density of neutrophils in the vicinity of intracortical blood injection was reported as ca. 200-400/mm^2 (Xue & Del Bigio, 2000). If it is assumed that each standard 5μm tissue section contains the same number of neutrophils, then a volume of 1μl would contain 40,000-80,000 neutrophils, so that 4μl would contain 160,000-320,000 neutrophils. To mimic these conditions, we therefore chose to inject 250,000 neutrophils in 4μl. The in vivo procedure resulted in a significant reduction in permeability when untreated neutrophils were compared with activated cells (fig 5), as well as a trend to reduced permeability when the per rat data was examined (fig 4). Perhaps of equal significance is the observation that none of the groups of neutrophils (untreated or activated) generated significant increases in permeability over that generated around the hematoma itself, although increases were possible as shown for the positive control (arachidonic acid, figs 3-5). As we have suggested, this data suggests a possible beneficial role for extravasated neutrophils in the mitigation of permeability increases during the acute stages of hematoma formation. However this study does not determine if these effects only apply to small hematomas, or if the effect is restricted to the milieu associated with the earliest stages of injury. Perhaps those neutrophils that diapedese into the brain around the hematoma site would exert different effects that are either dependent on hematoma size or on direct

16

neutrophil-endothelial interactions. The latter point is not addressed by the in vivo portion of this study. However, untreated neutrophils do reduce permeability as they come into contact with the endothelium according to our in vitro data (fig 2B).

The similarity of results in the in vitro system helps to validate the use of injecting human neutrophils into the rat model. It is likely that soluble factors such as reactive oxygen species are involved in the regulation of permeability by neutrophils, and these soluble factors would operate across different species. From a practical perspective, we chose to inject human neutrophils into the rat because of technical difficulties in extracting sufficient numbers of neutrophils from rat blood. Methods used by other investigators involve increasing rat neutrophils by using inflammatory stimuli, or by direct extraction from bone marrow, but both methods would make it difficult to extract relatively quiescent neutrophils. This would have interfered with our aim to compare responses between untreated and activated neutrophils. The histological sections were obtained to confirm that neutrophils were present in the sections used to generate permeability maps. However the thickness of the sections (30μm) as well as the admixture of neutrophils and red blood cells (see fig 3) prevented the sections being used to measure the distance between neutrophils and surrounding microvessels.

The in vivo data can be used to estimate an equivalent permeability coefficient for Horseradish peroxidase (HRP), and by extension, to the smaller molecule Lucifer yellow. This is of interest because Lucifer yellow was used in other studies by our group to measure permeability changes across inflamed pial microvessels in the same age and species of rat (Easton & Fraser, 1994). To estimate HRP permeability, the data was divided by $142 cm^2/g$, the surface area of microvessels

17

measured in rat striatum (Schlageter et al, 1999). If HRP and Lucifer yellow diffuse freely through the same permeability pore, the values may be multiplied by the ratio of the free diffusion coefficients for the two molecules (9.81) to obtain an estimate of Lucifer Yellow permeability ($Pest_{LY}$). While this is an assumption, it can be based on the observation that values for Lucifer yellow and albumin permeability (albumin has a similar size to HRP) in inflamed cerebral microvessels do approximate to this ratio (Easton & Fraser, 1994). For the per rat data shown in fig 2 $Pest_{LY}$ is $7.77 \pm 2.70 \times 10^{-6}$ cm/s for saline, $4.08 \pm 1.87 \times 10^{-6}$ cm/s for untreated neutrophils, $6.22 \pm 1.61 \times 10^{-6}$ cm/s around activated neutrophils and $34.53 \pm 6.55 \times 10^{-6}$ cm/s for arachidonic acid. The latter can be compared to our work on the effect of arachidonic acid in single pial microvessels. Mean P_{LY} induced by 10^{-3} mol/l arachidonic acid in pial microvessels was $12.61 \pm 3.44 \times 10^{-6}$ cm/s (Easton & Fraser, 1998), which is the same order of magnitude as our estimate in this study. This value is also within the range of actual P_{LY} observed in the single vessels (0.65-63.51×10^{-6} cm/s). This supports the notion (proposed by Gauden et al (2007)) that responses are comparable between smaller pial microvessels (diameter under 30μm) and vessels in the parenchyma. This is an important observation, because it is often argued that responses in pial microvessels do not reflect changes seen in the brain as a whole. This analysis also validates the technique used to measure permeability in this study.

Conclusion.

In a wider context, the role of neutrophils in the pathogenesis of BBB disruption and vasogenic cerebral edema is controversial. This study shows that relatively quiescent neutrophils can reduce BBB permeability, and suggests that neutrophil activation alone is not sufficient to induce net disruption of the BBB. The in vivo model has limited application to acute intracerebral

18

hemorrhage and the role of extravasated neutrophils early in this disease, but the significance of

our findings in the broad context of cerebral disease remains to be determined.

4. Experimental procedures.

Materials.

Unless otherwise stated, all reagents were obtained from Sigma-Aldrich (Missisauga, ON). Arachidonic acid and leukotriene B_4 were dissolved as stock solutions in 100% ethanol. Solutions were freshly prepared by removing stock solution and evaporating the ethanol with a stream of 100% N_2 gas, immediately dissolving the residue in 0.1mol/l Na_2HCO_3. This was then diluted in saline (0.9% NaCl) before application to give a maximum final Na_2HCO_3 concentration of 1×10^{-3}mol/l.

Cell cultures.

The human brain endothelial cell line hCMED/D3 was generated by three of the authors (Drs Weksler, Couraud and Romero; Weksler et al, 2005) and kindly provided by Dr Weksler to Dr Easton's laboratory, where these studies were performed. The cells were recovered from liquid nitrogen at the 4th passage after subcultivation, and initially plated onto uncoated plastic in complete EGM-2MV medium (Microvascular Endothelial Cell Medium-2, Cambrex, Walkersville, MD). Complete medium consisted of EGM-2MV medium with added 2.5% fetal bovine serum and a supplement containing hydrocortisone and growth factors. The medium was replaced every 3-5 days, and cells reached confluency after 10-15 days. Cells were passaged using trypsin-EDTA (1X) for subsequent use in permeability experiments.

Neutrophil isolation, neutrophil activation assay.

Neutrophils were isolated from human donor venous blood, as previously described (Inglis et al, 2004), and used within 6h of isolation. 5×10^5 neutrophils were added to wells of a 96 well plate in 100µl aliquots, and the assay initiated by the addition of the reactive oxygen species (ROS) sensitive fluorescent dye carboxy-2',7'-dichlorodihydrofluorescein diacetate (10^{-5}mol/l; Invitrogen, Burlington, ON). Neutrophils were then combined with activating factors as detailed in the Results, and the final volume in the wells was brought up to 150µl with PBS. Fluorescence was recorded on a microplate reader (Fluoroskan Ascent FL, Thermo Electron, Vantaa, Finland) at 485nm (excitation) and 527 nm (emission) every 15min for 135min.

In vitro permeability measurements.

hCMEC/D3 were seeded onto collagen inserts (0.4µm pore size, Transwell, Corning-Costar, Fisher Scientific, Whitby, ON) in complete EGM-2MV medium at 5×10^5 cells/cm^2. Cells were grown to confluency over 10 days before use. Permeability was assessed from the clearance of fluorescein isothiocyanate (FITC) labeled dextran (4kd molecular weight). The inserts were placed in wells of 12 well plates. To measure permeability, FITC-dextran (5mg/ml) was added to the inserts, which were then transferred every 5min over 30min to a series of collecting wells containing 1.5ml of fresh medium. 100µl samples from the collecting wells were placed in a 96 well plate, and the dextran fluorescence determined on the microplate reader at 485nm (excitation) and 538nm (emission). Fluorescence was converted to concentration using a standard curve. The volume cleared was calculated from the ratio of dextran concentration in each sample to the applied concentration (5mg/ml). The incremental cleared volume was plotted against time and the slope of the regression line through the data used to calculate a permeability-surface area (PS) value. PS for the endothelial monolayer (PS_e) was calculated

from $1/PS_e = 1/PS_t - 1/PS_b$, where PS_t is the regression slope across a test insert and PS_b the

regression slope across a blank (cell free) insert (Dehouck et al, 1992). PS_e values were divided

by the surface area of the insert ($1.13cm^2$) to derive the endothelial permeability coefficient, P_e

(cm/min).

Animals.

All animal procedures were approved by the Dalhousie University Committee on Laboratory

Animals, and comply with guidelines from the Canadian Council on Animal Care. Male Wistar

rats aged 30-35 days were purchased from Charles River (Saint-Constant, QB). Rats were

housed for a minimum of 5 days to acclimatize them prior to surgery, and were allowed free

access to pelleted food and water and kept on a 12 hour light/dark cycle.

Surgery.

Inhalational anesthesia was administered using isoflurane (4% induction, 2.5% maintenance) in

100% oxygen, and depth of anesthesia assessed by foot pinch reflex. Temperature was

maintained at 37°C with a heating pad and feedback system attached to a rectal probe (Fine

Science Tools, Vancouver, BC). A midline skin incision was made to expose the left jugular

vein. Retrograde cannulation was carried out using polyethylene tubing (I.D 0.58mm, O.D.

0.97mm, Fisher Scientific). The skin was sutured, and the animal placed prone, and its head

secured in a stereotactic frame (David Kopf Instruments, Tujunga, CA). An incision was made

through the scalp and the skull exposed by skin retraction. Two burr holes were positioned along

the coronal suture, 3.5mm on either side of the midline, using a dental drill (Fine Science Tools).

Injections (4μl) were then made through a 26 gauge metal needle inserted to a depth of 5mm

bilaterally. To obtain an internal control for each rat, neutrophils (2.5×10^5) were injected into the left striatum and a vehicle control (0.9% saline) or positive control (10^{-3}mol/l arachidonic acid) were injected into the right striatum. The needle rested for 1min before injecting at the rate of 0.5μl/min with a microinjection unit (David Kopf Instruments). The needle was left in place for 10min before removal to avoid back flux. Following the stereotactic injections, an interval of 15min elapsed during which those animals in which we intended to activate neutrophils received an intravenous injection of Leukotriene B_4 as detailed in the Results, while remaining groups were not treated further. After 15min, the animal was infused through the jugular vein with horseradish peroxidase (HRP type IV, 0.35 mg/g dissolved in 200 μl 0.9% saline), which circulated for 15min. Blood samples (100 μl) were taken from the jugular vein at 5, 10 and 15min after this infusion. At the end of the infusion period (15min), the rats were given a lethal dose (65mg/kg IV) of sodium pentobarbitone (CEVA Sante Animale, La Ballastiere, QC) and then perfused through the heart with 50ml saline containing sodium heparin (100U/ml, 4ºC) followed by 100ml 4% paraformaldehyde (PFA) in phosphate buffered saline (PBS, 50ml/3min with a Simon peristaltic pump, Stoeltingco, IL). A clamp was placed on the descending aorta to direct the perfusate towards the head, and the effluent drained through an incision in the right atrium. The brain was then removed from the skull by careful dissection and post fixed for 72h in 4% PFA. It was subsequently immersed in 30% sucrose for 48h to cryoprotect the tissue during sectioning on the freezing microtome.

Histology.

Brains were sliced in the coronal plane on a freezing microtome (Microm, Leica, USA) in alternating 30μm and 120μm sections and stored in 24 well plates in Millonig buffer solution

23

(containing 0.1mol/l NaH_2PO_4, 7.85 X 10^{-2}mol/l NaOH in distilled water, pH 7.2, 4°C) prior to

tissue processing. The 30μm sections were mounted on silinated glass slides (Fisher Scientific)

and stained with Mallory's hematoxylin and eosin (H&E). The H&E sections were used to

determine the size of the post-injection hematoma from the presence of red blood cells in the

needle tract, and to locate the injected neutrophils. Slides were examined by light microscopy

with a Nikon Eclipse E600 microscope. The volume of the hematoma was measured using

image analysis software (NIH Image J). Foci of hemorrhage were outlined in the H&E sections

to determine the surface area in mm^2. This was multiplied by the thickness of the section (30μm

or 0.03mm) to obtain a volume in μl (where 1μl=1mm^3). The volume was estimated in the

intervening 120μm sections by taking an average of the areas in the H&E sections immediately

anterior or posterior to the thicker section and multiplying this by the thickness. All of the

sections in each animal were analyzed to obtain a cumulative hematoma volume per rat. The

thicker 120μm sections were used to construct permeability-surface area (PS) maps.

Generation of in vivo permeability maps.

The method follows that published by Gauden et al (2007). The 120μm sections were mounted

onto silinated slides and reacted with diaminobenzidine (DAB, 8mg/ml) and hydrogen peroxide

(H_2O_2,0.006%), that combine with HRP to generate a brown reaction product. The tissue was

transilluminated during the reaction through a light box containing a uniform flat field light

source (3 piece LED, 3M), and sequential images captured every 5s for 200s through a

stereomicroscope (Leica S6D, Leica Microsystems, Richmond Hill, ON) connected to a camera

(Hamamatsu C4742-80-12AG, Quorum Technologies, Guelph, ON) with a firewire link to a

computer (Dell Canada, North York, ON), under the control of customized image processing

software (Image Hopper, Samsara Research, Dorking, UK). To generate images in which pixel values increased over time, images of absorption (A) were generated, defined as $A=\log(I_o/I_t)$ where I_o is intensity in the first image and I_t intensity in subsequent images at a given time, t. The initial image was divided by all subsequent images to create a stack of absorption images. The absorption series were then processed further to obtain a regression image through the initial images (0-35s). This regression image gives pixel values proportional to the initial rate of development of reaction product. Tissue and plasma calibrations were carried out to demonstrate that this initial rate is proportional to HRP concentration. Brains were obtained from rats perfused transcardially with heparinized saline and sectioned into cubes ($1cm^3$). These were incubated in horse serum containing streptomycin (10 µg/ml) and penicillin (20 U/ml) with different HRP concentrations for 30h at 37ºC in a static water bath (Electrothermal, England). These treatments had been shown to saturate the tissue to a depth of 500μm (Stewart et al., 1992). Cubes were then fixed in 4% PFA (72h), cryoprotected in 30% sucrose (48h) and sections taken within 500μm of the surface. The initial rate showed a linear relationship with tissue concentration (fig 1, supplementary information). Plasma calibrations were carried out by dissolving known concentrations of HRP in rat plasma taken from an untreated rat. 20µl of plasma was mixed with a 4ml mixture of DAB (4mg/ml) and H_2O_2 (0.006%) and immediately transferred to a Petri dish (3.5cm diameter) and placed on the light box to capture images. The initial rate increased in a linear manner with plasma HRP concentration (fig 2, supplementary information).

To convert a tissue concentration image into a map of permeability-surface area (PS) product, the image was divided by the time-integral product of plasma concentration, derived from the

25

HRP concentration in the blood samples taken at 5, 10 and 15min. This is based on a modified form of the Renkin-Crone equation where $PS=Q_r/\int(C_{pl})dt$, where Q_r is the amount of HRP in the tissue and $\int(C_{pl})dt$ is the time integral concentration of HRP in the plasma (Rapoport, 1978). The three values of plasma concentration were converted to a time integral value using statistical software (GraphPad Prism). The tissue concentration image was then divided by this value to obtain a PS map. The values generated by endogenous peroxidase were estimated using brain sections from sham operated rats, and subtracted from the sections. Over 15min, the HRP that enters the brain is expected to distribute in the interstitial space, with minimal uptake by surrounding cells. Therefore the image was further multiplied by a volume term that estimates the interstitial volume per gram of tissue ($0.2cm^3/g$, (Go, 1997)). Because the PS image contained many discrete regions, PS was calculated in individual regions of interest (ROI) outlined with a hand tool on Image Hopper. By assuming a tissue thickness of 120μm, and using the size of each pixel (19.87μm, obtained from images of metric divisions on a ruler), the volume in each ROI was calculated. The average PS in each ROI was multiplied by this volume to obtain a final PS value in ml/s/g. To ensure that the increase in signal was not due to endogenous peroxidase in the vicinity of the injection sites (in neutrophils or red blood cells), a subset of animals in each treatment group was processed without infusing HRP. Images from these brains did not show any discernable increase in signal above background under the conditions employed, ensuring that the signal observed was due to extravasated HRP and not cellular peroxidase. Other than background staining, signal was also not increased in the brains of sham operated animals infused with HRP. This indicated that signal was not increased from retained intravascular HRP due to incomplete flushing of the circulation (data not shown).

Statistics.

Data from each treatment group is expressed as mean ± standard error of the mean (sem).

Statistical comparisons between treatment groups were made using statistical software

(GraphPad Prism). Multiple groups were compared by one way analysis of variance followed by

the Tukey test. Histograms were compared using the X^2 test. P<0.05 was taken as significant.

References.

Adelson, P.D., Whalen, M.J., Kochanek, P.M., Robichaud, P., Carlos, T.M., 1998. Blood

brain barrier permeability and acute inflammation in two models of traumatic brain injury in the

immature rat: a preliminary report. Acta Neurochir Suppl 71, 104-106.

Ahmed, S.H., He, Y.Y., Nassief, A., Xu, J., Xu, X.M., Hsu, C.Y., Faraci, F.M., 2000.

Effects of lipopolysaccharide priming on acute ischemic brain injury. Stroke 31, 193-199.

Anthony, D.C., Bolton, S.J., Fearn, S., Perry, V.H., 1997. Age-related effects of

interleukin-1 beta on polymorphonuclear neutrophil-dependent increases in blood-brain barrier

permeability in rats. Brain 120, 435-444.

Anthony, D.C., Dempster, R., Fearn, S., Clements, J., Wells, G., Perry, V.H., Walker, K.,

1998. CXC chemokines generate age-related increases in neutrophil-mediated brain

inflammation and blood-brain barrier breakdown. Curr Biol 8, 923-926.

Barone, F.C., Hillegass, L.M., Tzimas, M.N., Schmidt, D.B., Foley, J.J., White, R.F., Price, W.J., Feuerstein, G.Z., Clark, R.K., Griswold, D.E., et al., 1995. Time-related changes in myeloperoxidase activity and leukotriene B4 receptor binding reflect leukocyte influx in cerebral focal stroke. Mol Chem Neuropathol 24, 13-30.

Berkow, R.L., Wang, D., Larrick, J.W., Dodson, R.W., Howard, T.H., 1987. Enhancement of neutrophil superoxide production by preincubation with recombinant human tumor necrosis factor. J. Immunol. 139, 3783-3791.

Cucullo, L., Couraud, P. O., Weksler, B., Romero, I. A., Hossain, M., Rapp, E., Janigro, D., 2008. Immortalized human brain endothelial cells and flow-based vascular modeling: a marriage of convenience for rational neurovascular studies. J. Cereb. Blood Flow Metab. 28, 312-328.

Dehouck, M.P., Jolliet-Riant, P., Bree, F., Fruchart, J.C., Cecchelli, R., Tillement, J.P. 1992. Drug transfer across the blood-brain barrier: correlation between in vitro and in vivo models. J. Neurochem. 58, 1790-1797.

Del Maschio, A., De Luigi, A., Martin-Padura, I., Brockhaus, M., Bartfai, T., Fruscella, P., Adorini, L., Martino, G., Furlan, R., De Simoni, M.G., Dejana, E., 1999. Leukocyte recruitment in the cerebrospinal fluid of mice with experimental meningitis is inhibited by an antibody to junctional adhesion molecule (JAM). J Exp Med 190, 1351-1356.

Del Zoppo, G.J., Becker, K.J., Hallenbeck, J.M., 2001. Inflammation after stroke: is it harmful? Arch Neurol 58, 669-672.

Easton, A.S., Fraser, P.A., 1994. Variable restriction of albumin diffusion across inflamed cerebral microvessels of the anaesthetized rat. J. Physiol. 475, 147-157.

Easton, A.S., Fraser, P.A., 1998. Arachidonic acid increases cerebral microvascular permeability by free radicals in single pial microvessels of the anaesthetized rat. J. Physiol. 507, 541-547.

Forster, C., Burek, M., Romero, I. A., Weksler, B., Couraud, P. O., Drenckhahn, D., 2008. Differential effects of hydrocortisone and TNFalpha on tight junction proteins in an in vitro model of the human blood-brain barrier. J. Physiol. 586, 1937-1949.

Gauden, V., Hu, D.E., Kurokawa, T., Sarker, M.H., Fraser, P.A., 2007. Novel technique for estimating cerebrovascular permeability demonstrates capsazepine protection following ischemia-reperfusion. Microcirculation 14, 767-778.

Go, K.G., 1997. The normal and pathological physiology of brain water. Adv. Tech. Stand. Neurosurg. 23, 47-142.

Hartl, R., Medary, M., Ruge, M., Arfors, K.E., Ghajar, J., 1997. Blood-brain barrier breakdown occurs early after traumatic brain injury and is not related to white blood cell adherence. Acta Neurochir Suppl 70, 240-242.

Inglis, V.I., Jones, M.P., Tse, A.D., Easton, A.S., 2004. Neutrophils both reduce and increase permeability in a cell culture model of the blood-brain barrier. Brain Res. 998, 218-229.

Jenkins, A., Maxwell, W. L., Graham, D., 1989. Experimental intracerebral haematoma in the rat: sequential light microscopical changes. Neuropathol. Appl. Neurobiol. 15, 477-486

Keep, R. F., Xi, G., Hua, Y., Hoff, J. T., 2005. The deleterious or beneficial effects of different agents in intracerebral hemorrhage: think big, think small, or is hematoma size important? Stroke 36, 1594-1596.

Kitaoka, T., Hua, Y., Xi, G., Hoff, J. T., Keep, R.F, 2002. Delayed argatroban treatment reduces edema in a rat model of intracerebral hemorrhage. Stroke 33, 3012-3018.

Lindsberg, P.J., Carpen, O., Paetau, A., Karjalainen-Lindsberg, M.L., Kaste, M., 1996. Endothelial ICAM-1 expression associated with inflammatory cell response in human ischemic stroke. Circulation 94, 939-945.

Lo, W.D., Chen, R., Boue, D.R., Stokes, B.T., 1998. Effect of neutrophil depletion in acute cerebritis. Brain Res 802, 175-183.

Matsuo, Y., Onodera, H., Shiga, Y., Nakamura, M., Ninomiya, M., Kihara, T., Kogure, K., 1994. Correlation between myeloperoxidase-quantified neutrophil accumulation and ischemic brain injury in the rat. Effects of neutrophil depletion. Stroke 25, 1469-1475.

Palmblad, J., Gyllenhammar, H., Lindgren, J.A., Malmsten, C.L., 1984. Effects of leukotrienes and f-Met-Leu-Phe on oxidative metabolism of neutrophils and eosinophils. J. Immunol. 132, 3041-3045.

Rapoport, S.I., 1978. A mathematical model for vasogenic brain edema. J. Theor. Biol. 74, 439-467.

Reese, T.S., Karnovsky, M.J., 1967. Fine structural localization of a blood-brain barrier to exogenous peroxidase. J. Cell Biol. 34, 207-217.

Rubin, L.L., Hall, D.E., Porter, S., Barb, K., Canno, C., Horner, H.C., Janatpour, M., Liaw, C.W., Manning, K., Morales, J., Tanner, L.I., Tomaselli, K.J., Bard, F., 1991. A cell culture model of the blood-brain barrier. J. Cell Biol. 115, 1725-1735.

Schlageter, K.E., Molnar, P., Lapin, G.D., Groothuis, D.R., 1999. Microvessel organization and structure in experimental brain tumors: microvessel populations with distinctive structural and functional properties. Microvasc. Res. 58, 312-328.

Schurer, L., Prugner, U., Kempski, O., Arfors, K.E., Baethmann, A., 1990. Effects of antineutrophil serum (ANS) on posttraumatic brain oedema in rats. Acta Neurochir Suppl (Wien) 51, 49-51.

Sheppard, F.R., Kelher, M.R., Moore, E.E., McLaughlin, N.J., Banerjee, A., Silliman, C.C., 2005. Structural organization of the neutrophil NADPH oxidase: phosphorylation and translocation during priming and activation. J. Leukoc. Biol. 78, 1025-1042.

Simard, J.M., Kent, T.A., Chen, M., Tarasov, K.V., Gerzanich, V., 2007. Brain oedema in focal ischaemia: molecular pathophysiology and theoretical implications. Lancet Neurol. 6, 258-268.

Stewart, P.A., Farrell, C.R., Farrell, C.L., Hayakawa, E., 1992. Horseradish peroxidase retention and washout in blood-brain barrier lesions. J. Neurosci. Methods 41, 75-84.

Tauber, M.G., Borschberg, U., Sande, M.A., 1988. Influence of granulocytes on brain edema, intracranial pressure, and cerebrospinal fluid concentrations of lactate and protein in experimental meningitis. J Infect Dis 157, 456-464.

Weksler, B.B., Subileau, E.A., Perriere, N., Charneau, P., Holloway, K., Leveque, M., Tricoire-Leignel, H., Nicotra, A., Bourdoulous, S., Turowski, P., Male, D.K., Roux, F., Greenwood, J., Romero, I.A., Couraud, P.O., 2005. Blood-brain barrier-specific properties of a human adult brain endothelial cell line. Faseb J. 19, 1872-1874.

Whalen, M.J., Carlos, T.M., Kochanek, P.M., Clark, R.S., Heineman, S., Schiding, J.K., Franicola, D., Memarzadeh, F., Lo, W., Marion, D.W., Dekosky, S.T., 1999. Neutrophils do not mediate blood-brain barrier permeability early after controlled cortical impact in rats. J Neurotrauma 16, 583-594.

Wispelwey, B., Lesse, A.J., Hansen, E.J., Scheld, W.M., 1988. Haemophilus influenzae lipopolysaccharide-induced blood brain barrier permeability during experimental meningitis in the rat. J Clin Invest 82, 1339-1346.

Wong, D., Prameya, R., Dorovini-Zis, K., 2007. Adhesion and migration of polymorphonuclear leukocytes across human brain microvessel endothelial cells are differentially regulated by endothelial cell adhesion molecules and modulate monolayer permeability. J. Neuroimmunol. 184, 136-148.

Xue, M., Del Bigio, M. R., 2000. Intracortical hemorrhage injury in rats: relationship between blood fractions and brain cell death. Stroke 31, 1721-1727.

Yamasaki, Y., Matsuo, Y., Matsuura, N., Onodera, H., Itoyama, Y., Kogure, K., 1995. Transient increase of cytokine-induced neutrophil chemoattractant, a member of the interleukin-8 family, in ischemic brain areas after focal ischemia in rats. Stroke 26, 318-322.

Zhang, R.L., Chopp, M., Chen, H., Garcia, J.H., 1994. Temporal profile of ischemic tissue damage, neutrophil response, and vascular plugging following permanent and transient (2H) middle cerebral artery occlusion in the rat. J Neurol Sci 125, 3-10.

Figure legends.

Figure 1. Permeability responses in the human brain endothelial cell line hCMEC/D3. Cells were pre-treated for 24h with dibutyryl cyclic AMP (dbcAMP, 2.5×10^{-4} mol/l) and rolipram (1.75×10^{-5} mol/l) or treated acutely with arachidonic acid (AA, 0.5×10^{-3} mol/l). The resultant permeability is shown as mean ± sem (standard error of the mean), n values indicated. Significance is compared to untreated cells (baseline), $*P<0.05$, $**P<0.01$.
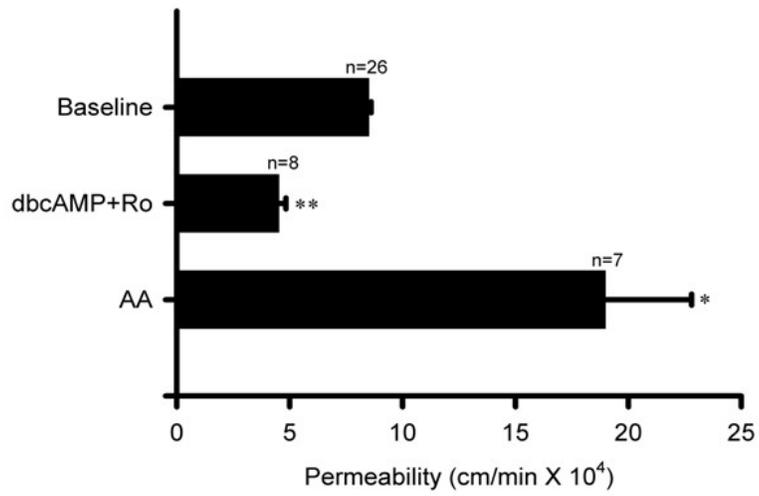
Figure 2. In vitro effects of neutrophil activation. A. Neutrophil activation assay. Change in fluorescence over 135min in neutrophils (PMN) loaded with the reactive oxygen species (ROS) sensitive fluorescent dye carboxy-2',7'-dichlorodihydrofluorescein diacetate. PMN were treated with tumor necrosis factor (100U/ml, +TNF), leukotriene B_4 (10^{-7} mol/l, +LtB$_4$), alone or combined (+TNF+LtB$_4$), phorbyl 12-myristate, 13-acetate (4×10^{-8} mol/l, +PMA) alone or combined with diphenylene iodinium chloride (DPI, 8×10^{-6} mol/l, +PMA+DPI). Vehicle (phosphate buffered saline, PBS) and DPI were also tested alone. B. Permeability changes in hCMEC/D3. Permeability is normalized to baseline permeability in untreated monolayers (expressed as % of baseline). Neutrophils were either applied without treatment (untreated), exposed to a gradient of LtB$_4$ (10^{-7} mol/l, LtB$_4$ below), activated with TNF (100U/ml) and LtB$_4$ (10^{-7} mol/l, activated) or activated in the presence of ROS scavengers (superoxide dismutase 10U/ ml and catalase 1000U/ml, S+C). As a control, LtB$_4$ (10^{-7} mol/l, LtB$_4$ alone) was applied without neutrophils. Data is expressed as mean ± sem. Significance is compared to baseline or to conditions linked by cross bars (ns=not significant, $*P<0.05$, $**P<0.01$, $***P<0.001$).

Figure 3. Permeability maps around striatal injections of (A) activated neutrophils and (B) arachidonic acid (10^{-3}mol/l) into an acute hematoma. Upper and lower panels show H&E stained sections (30μm) taken anterior (upper) and posterior (lower) to the thicker section (120μm) used to generate a permeability map (middle panels). Brain hemisections (left) are shown with a highlighted region (box) magnified at right. The permeability map is pseudocolored to indicate graded values of permeability-surface area (PS) product for horseradish peroxidase. Scale bar=200μm.

Figure 4. PS (permeability-surface area) values in the acute hematoma around neutrophils (untreated or activated), vehicle (saline) alone or arachidonic acid (10^{3}mol/l). Data is mean ± sem, each data point is compiled for a separate rat (n as indicated). Significance is compared to vehicle or between treatments linked by cross bars (ns=not significant, ***$P<0.001$).

Figure 5. Histograms for PS values in individual regions of interest in the permeability maps from all of the rats, related to neutrophils (untreated or activated), vehicle (saline) alone or arachidonic acid (10^{-3}mol/l). The number of regions analyzed is shown (n) for each group. X^2 analysis was used to assess significance relative to activated neutrophils (when P is shown this indicates a significant difference, ns=not significant).
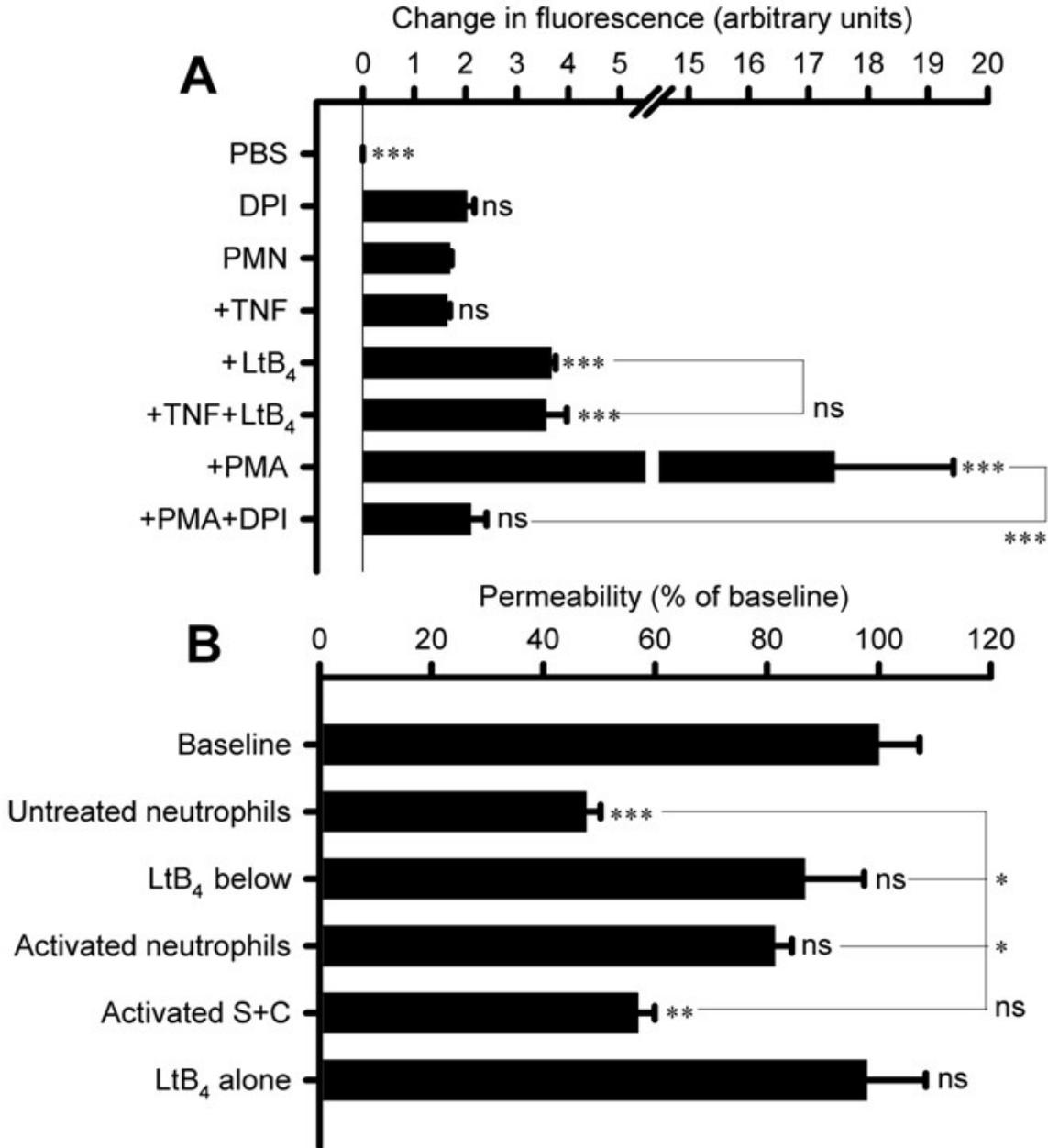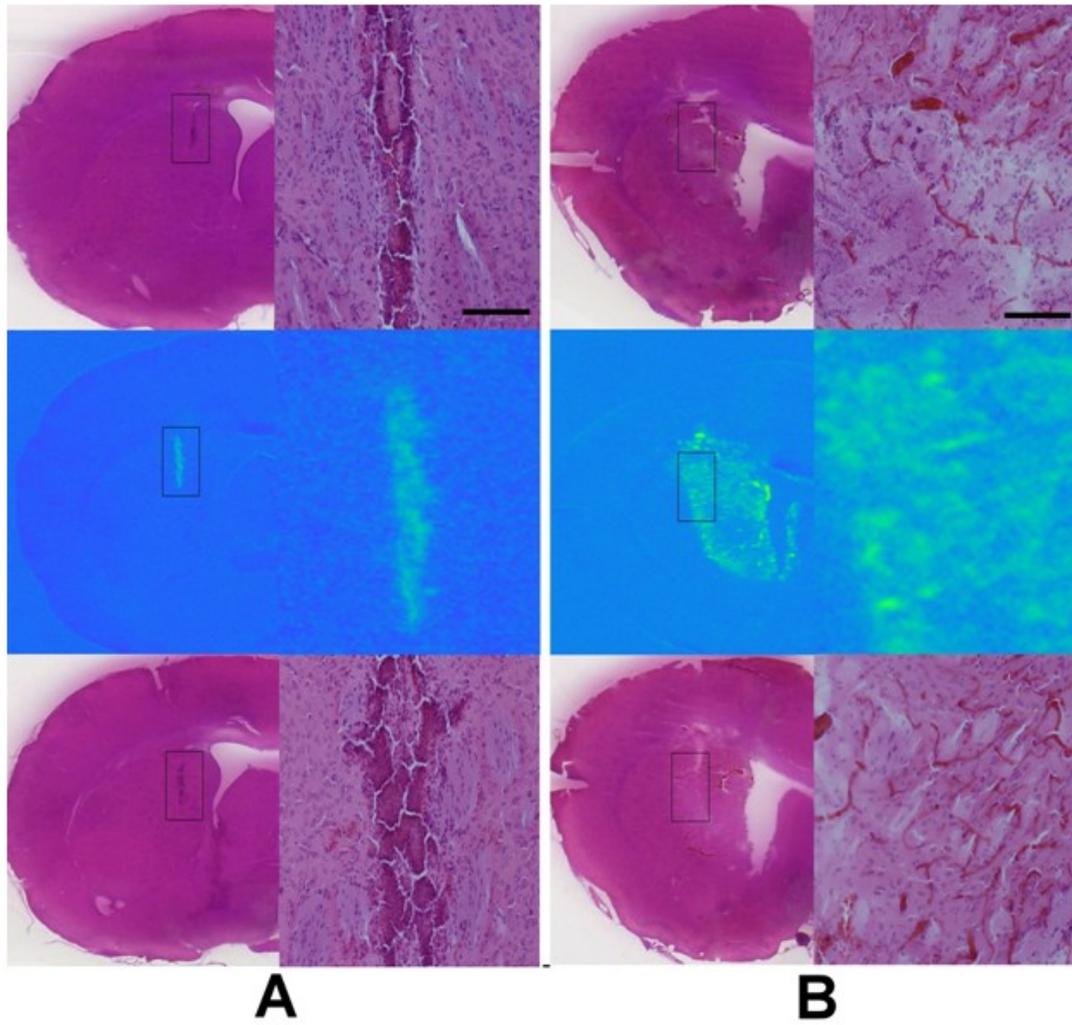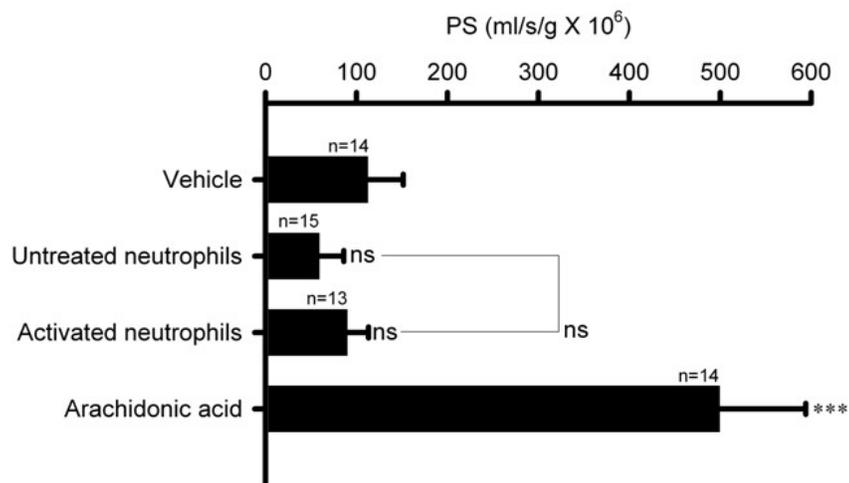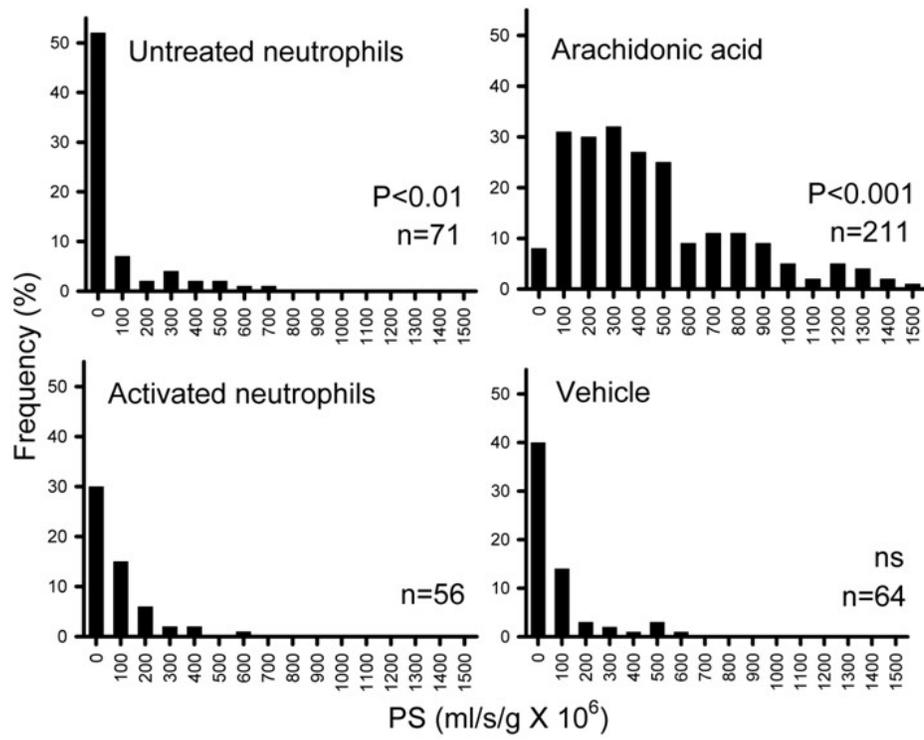
Figure 1

Figure 2

A   B

Figure 3

Figure 4

Figure 5